Chapter 7
Stellar Driven Evolution of Hydrogen-Dominated Atmospheres from Earth-Like to Super-Earth-Type Exoplanets

Kristina G. Kislyakova, Mats Holmström, Helmut Lammer, and Nikolai V. Erkaev

Abstract In the present chapter we discuss the impact of a host stars radiation and plasma environment to the escape and evolution of hydrogen-dominated exoplanet atmospheres. We focus mainly on planets within the Earth- to super-Earth mass domain and consider both, thermal and nonthermal atmospheric escape processes. The type of thermal loss mechanism depends on the so-called escape parameter, which is the ratio of the gravitational energy of a particle to its thermal energy. For low values of this parameter a planetary atmosphere switches from classical Jeans to modified Jeans escape and finally to hydrodynamic blow off. During blow off the majority of the atmospheric particles dispose of enough energy to escape the planet's gravity field. This leads to extreme gas losses. It is shown that non-thermal losses for light species such as hydrogen never exceed blow off escape, but they are of significant importance for planets with relatively weak Jeans-type escape or heavier particles (e.g., O, C, N). From the diversity of non-thermal escape mechanisms, in the present chapter we focus on ion pick-up and discuss the importance of other loss mechanisms. The general conclusion of the chapter is, that escape processes strongly shape the evolution of exoplanet atmospheres and determine, if the planet loses its hydrogen and/or volatile-rich protoatmospheres or, on the contrary, remains

K.G. Kislyakova (✉) • H. Lammer
Austrian Academy of Sciences, Space Research Institute, Graz, A-8042, Austria
e-mail: kristina.kislyakova@oeaw.ac.at; helmut.lammer@oeaw.ac.at

M. Holmström
Swedish Institute of Space Physics, P.O. Box 812, SE-98128 Kiruna, Sweden
e-mail: matsh@irf.se

N.V. Erkaev
Institute for Computational Modelling, 660041 Krasnoyarsk 36, Russia

Russian Academy of Sciences, and Siberian Federal University, 660041 Krasnoyarsk, Russian Federation
e-mail: erkaev@icm.krasn.ru

H. Lammer, M. Khodachenko (eds.), *Characterizing Stellar and Exoplanetary Environments*, Astrophysics and Space Science Library 411,
DOI 10.1007/978-3-319-09749-7_7

as a mini-Neptune, which can probably not be considered as a potential habitat as we know it.

7.1 Introduction: Hydrogen-Rich Terrestrial Exoplanets

One of the most important questions still awaiting the solution in the present-day exoplanetary science is the determination of possible evolution scenarios of exoplanets, which could explain all currently observed types. All exoplanets as well as planets in the Solar System experience atmospheric mass losses. There exist a number of observations and measurements of losses from Solar System terrestrial planets (see, for example, Lundin 2011), and observations in the Lyman-α line for the hot Jupiters HD 209458b and HD 189733b (Vidal-Madjar et al. 2003; Lecavelier des Etangs et al. 2010) and a hot Neptune GJ 436b (Kulow et al. 2014), (see also Chap. 4, Fossati et al. 2014). Excess absorption in Lyman-α is usually explained as an observational evidence for mass loss (Bourrier and Lecavelier des Etangs 2013).

Here we focus on Earth-size to super-Earth type planets (we call them terrestrial in the present chapter), i.e., we exclude massive exoplanets from consideration. According to present-day modeling, terrestrial-sized planets should be common in the Universe (Broeg 2009). We make a short review about the atmospheric evolution of these moderate size planets and factors, which define it, as it is understood at present.

The atmosphere mass and composition of a terrestrial planet is defined, first, by the formation conditions and, second, by the following stellar-driven escape processes. Atmospheres may take origin in the primordial nebula, where all exoplanets are believed to be born (Ikoma and Genda 2006; Lammer et al. 2013a, 2014), or be later outgassed from the planetary interiors during solidification of magma oceans (Elkins-Tanton and Seager 2008). In the second case one speaks about a secondary atmosphere. Both types of atmosphere formation are believed to be important and work together on the atmosphere evolution.

Tables 7.1 and 7.2 show modeling results of modelled gravitational attraction and accumulation of nebula gas around an Earth-mass and a super-Earth core inside the habitable zone (HZ) of a solar-like host star as a function of protoplanetary nebula

Table 7.1 Captured hydrogen envelopes from a protoplanetary nebula around an Earth-size exoplanet within the HZ of a solar-like star with a protoplanet core mass of $1M_{\oplus}$ in units of EO_H ($1EO_H = 1.53 \times 10^{23}$ g), for nebula conditions with dust depletion factors f_d of 0.001, 0.01, and 0.1 and relative accretion rates $\frac{\dot{M}_{acc}}{M_{pl}}$ between 10^{-5} and 10^{-8} year^{-1} (Lammer et al. 2014)

$\frac{\dot{M}_{acc}}{M_{pl}}$ [year^{-1}]	$f_d = 0.001$	$f_d = 0.01$	$f_d = 0.1$
10^{-5}	9.608 EO_H	1.682 EO_H	0.316 EO_H
10^{-6}	44.6 EO_H	12.8 EO_H	2.313 EO_H
10^{-7}	210.0 EO_H	65.75 EO_H	16.8 EO_H
10^{-8}	1002 EO_H	332.6 EO_H	93.2 EO_H

Table 7.2 Captured hydrogen envelopes from a protoplanetary nebula around a super-Earth with a core size of $1.71 R_{\oplus}$ and a core mass of $5 M_{\oplus}$ in units of EO_H ($1EO_H = 1.53 \times 10^{23}$ g), for nebula conditions with dust depletion factors f_d of 0.001, 0.01, and 0.1 and relative accretion rates $\frac{\dot{M}_{acc}}{M_{pl}}$ between 10^{-5} and 10^{-8} year^{-1} (Lammer et al. 2014)

$\frac{\dot{M}_{acc}}{M_{pl}}$ [year^{-1}]	$f_d = 0.001$	$f_d = 0.01$	$f_d = 0.1$
10^{-5}	956.2 EO_H	299 EO_H	170 EO_H
10^{-6}	4653 EO_H	1600 EO_H	690 EO_H
10^{-7}	28620 EO_H	8117 EO_H	3250 EO_H
10^{-8}	105816 EO_H	103725 EO_H	17810 EO_H

parameters such as dust grain depletion factor f_d and protoplanetary luminosity during accretion. The results are based on a model that solves the hydrostatic structure equations for the protoplanetary nebula (Lammer et al. 2014). Depending on nebular properties, such as f_d, planetesimal accretion rates, and resulting luminosities one can see that an Earth-like rocky core can capture hydrogen from a few percent of the hydrogen amount in an Earth Ocean (EO_H) of up to several 10 s to even 1,000 EO_H (see also Lammer et al. 2014). Compared to a core with an Earth-mass, the super-Earth core with $5 M_{\oplus}$ captures orders of magnitude more hydrogen. Even for a nebula condition with a high accretion rate and dust grain depletion factor the super-Earth would capture $\sim$170 EO_H. For low accretion rates an a $f_d = 0.001$ the planet would capture more than 10^5 EO_H. Thus, hydrogen envelopes that contain more than 1,000 EO_H may be common at super-Earths.

Recent findings of ESO's High Accuracy Radial velocity Planetary Searcher (HARPS) project and NASA's Kepler space observatory reveal from the radius-mass relation and the resulting density of discovered super-Earth, that these bodies probably have rocky cores, but are surrounded by significant H/He, H_2O envelopes, or both (e.g., http://www.exoplanet.eu). These findings demonstrate, that even if an exoplanet has a terrestrial size, its evolution may still differ much from the one of the Earth leaving the planet as a mini-Neptune type body. These discoveries raise the question about different evolution scenarios these exoworlds went and demonstrate, that not all of them could rid of their primordial dense envelopes. After the atmosphere formation is completed, its loss and evolution are defined by intensity of escape processes.

Several types of escape mechanisms from planetary atmospheres are known. The light gases like H and He are the most inclined to escape, however, heavier species can be lost too. It was shown by several authors such as Tian et al. (2008a,b), Lichtenegger et al. (2010), Lammer et al. (2013a), that nitrogen-dominated atmospheres are not easy to be kept during the first extreme phases of the star's activity after it's arrival at ZAMS due to extreme atmospheric expansion. Other species can be lost due to drag with the escaping hydrogen (this is considered as a possible explanation for Xe fractionation in the atmosphere of the Earth and was estimated, e.g., by Hunten et al. 1987). CO_2 atmosphere should not experience such strong expansion (Kulikov et al. 2006) and could be kept more easily, as one may see in the case of Venus.

Roche lobe effects can play a very important role for inflated close-in exoplanets, which fill their Roche lobe and consequently lose big amounts of mass (e.g. Erkaev et al. 2007; Lecavelier des Etangs et al. 2004). Close-in terrestrial planets lose their primordial hydrogen envelopes relatively easy (Leitzinger et al. 2011) and develop into hot bodies without atmosphere like CoRoT-7b. However, it is not so clear how mediate-sized planets in sub- to super-Earth mass and size domain can evolve in the HZs of their stars. Can they often evolve to Class I habitats with nitrogen atmosphere and life favorable conditions (Lammer et al. 2009a) which resemble the Earth, or do they usually evolve differently?

In this chapter we present the summary of our evolutionary studies for hydrogen-rich terrestrial-type exoplanets located in the HZ of its parent star. We consider thermal and nonthermal ion pick-up losses and discuss their possible influence on the planetary evolution. The main aim is to estimate the conditions under which these primordial hydrogen envelopes may be lost, leaving back an exoplanet with a possible Earth-type atmosphere.

7.2 Thermal Escape

On the basis of the sources of the host stars soft X-ray and EUV energy (XUV) input into the upper atmosphere, one can separate two main escape categories: thermal escape of neutral particles and non-thermal escape of neutrals and ions. Jeans escape is the classical thermal escape mechanism based on the fact that the atmospheric particles have velocities according to the Maxwell distribution. Figure 7.1 illustrates upper atmosphere processes and its response to solar/stellar XUV radiation (see also Chap. 6, Shematovich et al. 2014). Individual particles in the high tail of the distribution may reach escape velocity at the exobase altitude, where the mean free path is comparable to the scale height, so that they can escape from the planet's atmosphere. When the thermosphere temperature rises due to heating by the stellar XUV radiation, the bulk atmosphere starts hydrodynamically to expand with consequent adiabatic cooling. In such a case the velocity distribution at the exobase level is described by a shifted Maxwellian (e.g., Tian et al. 2008a, Erkaev et al. 2013). This regime can be called controlled hydrodynamic escape which resembles a strong Jeans-type escape but is still weaker compared to classical blow-off, where no control mechanism influences the escaping gas. If the XUV heating continues to increase so that the ratio between the gravitational and thermal particle energy becomes ≤ 1.5 than so-called blow off occurs leading to a stronger escape in comparison to the Jeans and even the controlled hydrodynamic escape. As it is shown by Erkaev et al. (2013), depending on the availability of possible IR-cooling molecules and the planets average density, hydrogen-rich super-Earths orbiting inside the HZ will reach hydrodynamic blow-off only for XUV fluxes several 10 times higher compared to today's Sun, which is the case for the early evolution of a Solar-type star (Güdel 2007). Most of their lifetime the upper atmospheres of these planets will experience non-hydrostatic conditions, but not blow off. In such

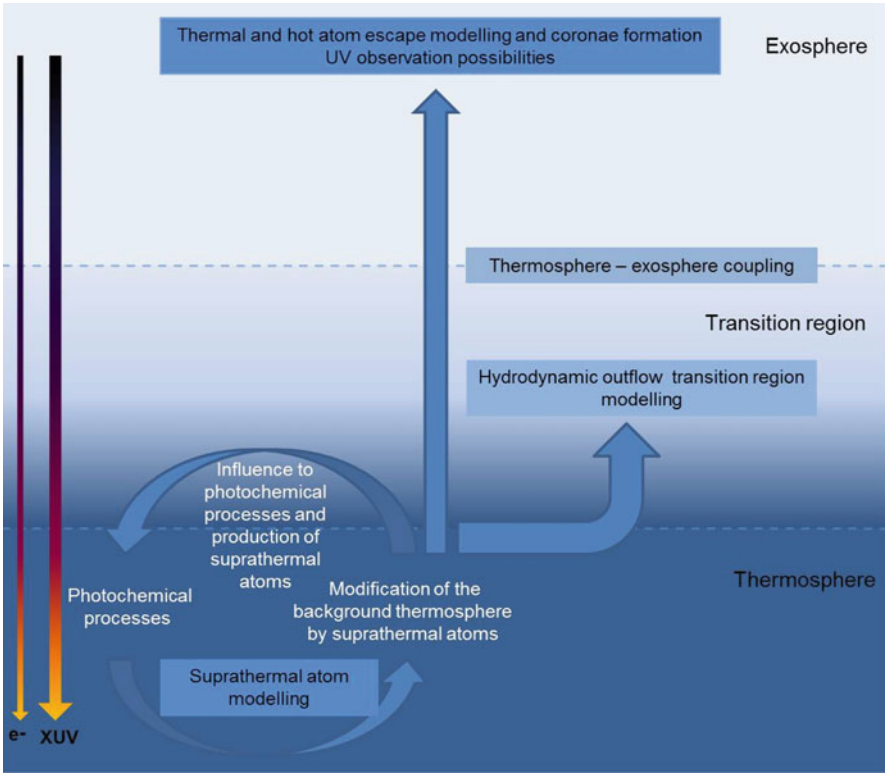

Fig. 7.1 Illustration of processes that occur in the upper atmosphere of planets. Heating by solar/stellar XUV radiation, photoelectrons, photochemical processes and the production of suprathermal atoms will modify the thermosphere structure and vice versa (see also Chap. 6, Shematovich et al. 2014). The temperature at which the transition from hydrostatic to hydrodynamic conditions occurs depends on the composition of the thermosphere and will also be affected by efficient non-thermal escape processes. The escape of suprathermal particles in turn depends on the physical structure of the thermosphere and its temperature

case the upper atmosphere expands hydrodynamically and the loss of the upward flowing gas results in controlled hydrodynamic escape. The blow off stage is more easily reached at less massive hydrogen-rich planets with mass equal to that of the Earth. These planets experience hydrodynamic blow off for much longer, and change from the blow off regime to the controlled hydrodynamic escape regime for XUV fluxes which are $\leq$10 times of today's Sun. Because of XUV heating and expansion of their upper atmospheres, both an exo-Earth and a super-Earth should produce extended exospheres or hydrogen coronae distributed above possible magnetic obstacles defined by intrinsic or induced magnetic fields. In such case the hydrogen-rich upper atmosphere will not be protected by possible magnetospheres like on present-day Earth, but could be eroded by the stellar wind plasma flow and lost from the planet in the form of ions (Khodachenko et al. 2007; Kislyakova

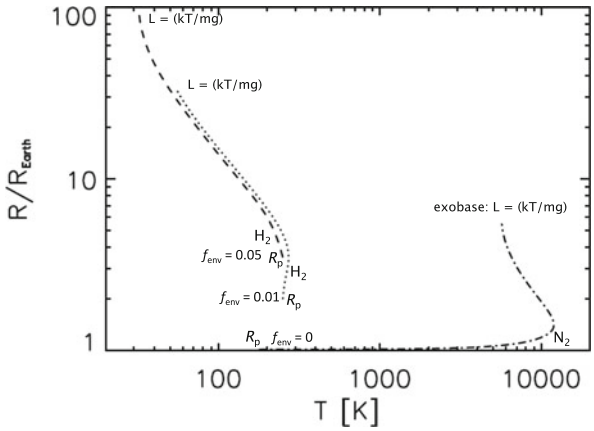

Fig. 7.2 Comparison of upper atmosphere temperature profiles for three Earth-like planets with core masses of 1 $M_{\oplus}$ that are exposed to a stellar XUV flux that is 10 times stronger compared to that of today's Sun. Two planets are surrounded by hydrogen envelopes f_{env} with $f_{env} = 0.01$ (*dotted line*) and 0.05 (*dashed line*). The third planet has an Earth-like nitrogen dominated atmosphere. The upper part of the profiles corresponds to the exobase level where the mean free path L of the atmosphere is similar as the scale height H

et al. 2013). Figure 7.2 shows three temperature profiles of planets with masses of $1M_{\oplus}$, but with different atmospheres. The profiles have been modeled with a hydrodynamic upper atmosphere and stellar XUV radiation absorption model that is described in detail in Erkaev et al. (2013). The dotted and dashed line correspond to Earth-mass planets with hydrogen envelopes f_{env}

$$f_{env} = \frac{M_{at}}{M_{at} + M_c}, \tag{7.1}$$

of 0.001 and 0.01, where M_{at} and M_c are the atmosphere and core masses and $R_p = R_c + z$ is the radius obtained from a transit. The third planet has an Earth-like nitrogen atmosphere with $f_{env} \sim 0$. In all three cases, the atmospheric masses are much lower than the core masses, so that $M_c \sim M_{pl} \sim M_{\oplus}$. However, according to Mordasini et al. (2012), Earth-mass planets with f_{env} of 0.001 and 0.01 have radii R_p that are much higher up in the atmosphere than their core radius R_c. The reason is that, in hydrogen atmospheres, visible light can not penetrate down to the surface (i.e., Jupiter, Saturn, Uranus, Neptune) because of Raleigh scattering (Lecavelier des Etangs et al. 2008). This is not the case for an Earth-like atmosphere. In a hydrogen dominated atmosphere, H_2 molecules are carriers of the Rayleigh scattering. The effective altitude at which the Rayleigh scattering of H2 molecules dominates depends on the mean density and as a consequence on the total pressure at the altitude. Because of this, the planetary radius R_p (see Fig. 7.2) corresponding to the atmospheric pressure P related to wavelength λ can then be written as

$$R_p = \frac{kT\mu g\tau^2}{P^2\sigma_{Rl}}, \tag{7.2}$$

with σ_{Rl} the λ dependent Rayleigh cross section, gravitational acceleration g, atmospheric temperature T, optical depth τ, the mean mass of atmospheric particles μ, and Boltzmann constant k. Therefore, for the two hydrogen-dominated protoplanets shown in Fig. 7.2, R_p will be larger in comparison to their core radii R_c and the nitrogen-rich planet case. This will result in the different average densities of the three planets shown in Fig. 7.2, although their masses are the same.

One can also see in Fig. 7.2, that if heated by the stellar XUV radiation that is 10 times higher compared to that of the present Sun, the temperature of the nitrogen atmosphere exceeds the one of the hydrogen atmospheres. The main reason is that the adiabatic cooling due to the hydrodynamic expansion is more effective in case of the hydrogen dominated upper atmosphere. One can also see from Fig. 7.2 that XUV exposed upper atmospheres can expand to several planetary radii. The profile curves end at the corresponding exobase levels where the mean free path L of the gas reaches the scale hight $H = kT/mg$, where m is the mean mass of the atmospheric species.

In this part of the chapter, calculations of the losses of captured hydrogen envelopes from protoplanets having masses in a range between Earth-like bodies and super-Earths with $5M_\oplus$ are presented by assuming that their rocky cores had formed before the nebula gas dissipated. In the thermal escape calculations we focused at bodies within the habitable zone (HZ) of a G star. These results are published in Lammer et al. (2014). This article is a continuation of the research performed by Erkaev et al. (2013), where the same methods were used to estimate the amount of hydrogen an Earth-type planet and a super-Earth ($M = 10M_\oplus$, $R = 2R_\oplus$) can lose in a HZ of a G star. The same code was also used by Lammer et al. (2013b) to estimate the thermal losses from 5 Kepler-11 super-Earths.

The model solves the system of the hydrodynamic equations for mass,

$$\frac{\partial \rho r^2}{\partial t} + \frac{\partial \rho v r^2}{\partial r} = 0, \tag{7.3}$$

momentum,

$$\frac{\partial \rho v r^2}{\partial t} + \frac{\partial \left[r^2(\rho v^2 + P)\right]}{\partial r} = -\rho g r^2 + 2Pr, \tag{7.4}$$

and energy conservation

$$\frac{\partial r^2 \left[\frac{\rho v^2}{2} + \frac{P}{(\gamma-1)}\right]}{\partial t} + \frac{\partial v r^2 \left[\frac{\rho v^2}{2} + \frac{\gamma P_p}{(\gamma-1)}\right]}{\partial r} = -\rho v r^2 g + q_{XUV} r^2. \tag{7.5}$$

Table 7.3 Thermal escape of hydrogen envelopes f_{env} in units of EO_H ($1EO_H = 1.53 \times 10^{23}$ g) from an Earth-size and mass planet inside the HZ according to a stellar XUV flux that is 100 times higher compared to that of the present Sun at 1 AU. Δt is the assumed exposure time, and z the envelope corresponding core-surface-radius distance (Mordasini et al. 2012; Lammer et al. 2014)

f_{env}	$z\,[R_\oplus]$	$\Delta t = 50$ Myr	$\Delta t = 100$ Myr	$\Delta t = 500$ Myr	$\Delta t = 1{,}000$ Myr
0.001	0.15	0.95 EO_H	1.9 EO_H	9.5 EO_H	19 EO_H
0.01	1	9.5 EO_H	19 EO_H	96.5 EO_H	193 EO_H

Table 7.4 Thermal escape of hydrogen envelopes f_{env} in units of EO_H ($1EO_H = 1.53 \times 10^{23}$ g) from a super-Earth with a core size of $1.71R_\oplus$ and a core mass of $5M_\oplus$ inside the HZ of its host star, according to a stellar XUV flux that is 100 times higher compared to that of the present Sun at 1 AU. Δt is the assumed exposure time, and z the envelope corresponding core-surface-radius distance (Mordasini et al. 2012; Lammer et al. 2014)

f_{env}	$z\,[R_\oplus]$	$\Delta t = 50$ Myr	$\Delta t = 100$ Myr	$\Delta t = 500$ Myr	$\Delta t = 1{,}000$ Myr
0.001	1.2	3.5 EO_H	6.9 EO_H	34.5 EO_H	69 EO_H
0.01	1.5	4.5 EO_H	9 EO_H	45 EO_H	90 EO_H
0.1	4	22.4 EO_H	44.7 EO_H	223.7 EO_H	447.5 EO_H

Here, r is the radial distance from the center of the protoplanetary core, ρ, P, T, v are the mass density, pressure, temperature and velocity of the nonhydrostatic outward flowing bulk atmosphere. γ is the polytropic index, g the gravitational acceleration and q_{XUV} is the XUV volume heating rate.

Tables 7.3 and 7.4 show the loss of protoplanetary nebula captured hydrogen envelopes due to hydrodynamic escape from an Earth-like core and a super-Earth with the size of a core size of $1.71R_\oplus$ and a core mass of $5M_\oplus$ inside the HZ of their host star in units of EO_H. The hydrogen envelopes are exposed to a XUV flux that is 100 times higher compared to that of today's Sun in 1 AU, a value expected during the early XUV saturation phase Δt of a young solar-like star (see also Chap. 1, Linsky and Güdel (2014)). Δt for G stars is expected to last about 100 Myr. It can be less for F stars but lasts longer for M dwarfs. The calculations have been performed in the domain from the lower thermosphere up to a critical point R_{crit}, where the Knudsen number equals to 0.1. The escape rates have been calculated with a heating efficiency of 15 % (see also Chap. 6, Shematovich et al. 2014). The escape of hydrogen from super-Earths can be large because of their large radii, bit it is too weak to evaporate the amount of captured hydrogen shown in Table 7.2, even if the exposure time equals 10^3 Myr. As it was shown by Erkaev et al. (2013) and Kislyakova et al. (2013), if an exoplanet located in the HZ does not lose the dense primordial hydrogen envelope during the first 90 Myr years of star's early XUV saturation period, it is unrealistic that the remaining gaseous envelope will be lost during the rest of the planet's lifetime. This can lead to the formation of a mini-Neptune instead of a super-Earth. Only close-in massive rocky planets such as CoRoT-7b (e.g., Leitzinger et al. 2011), that are exposed over a long time

period to high XUV fluxes, or that grow to large massive bodies after the nebula evaporated, can lose their hydrogen envelopes completely (Lammer et al. 2014). From the results of these studies one finds that the nebula properties, protoplanetary growth time, planetary mass, size and the host stars radiation environment are the initial conditions, which define if the planets can evolve to the Earth-like class I habitats (Lammer et al. 2009a). Protoplanets with core masses that are $\leq 1 M_{\oplus}$ can lose their captured hydrogen envelopes during the active XUV saturation phase of their host stars inside the HZ of solar-like stars (Lammer et al. 2014), while rocky cores within the so-called super-Earth domain most likely can not get rid of their nebula captured hydrogen envelopes during their whole lifetime. Our results are in agreement with the suggestion that Solar System terrestrial planets, lost their nebula-based protoatmospheres during the XUV activity saturation phase of the young Sun. The results of these models are also in agreement with the discovery of low density hydrogen and/or volatile-rich super-Earths even at closer orbital distances <1 AU. These findings indicate that these planets could not lose their primordial atmospheres (see Fig. 13.1, Chap. 13, Fridlund et al. 2014). Furthermore, the results of these studies indicate that one should expect that many mini-Neptunes may populate the HZs of solar-like stars.

7.3 Ion Pick-Up

Besides thermal escape, various non-thermal escape mechanisms also contribute to the total mass loss and have to be accounted for. Non-thermal escape processes can be separated into ion escape and photochemical and kinetic processes that accelerate atoms beyond escape energy. Ions can escape from an upper atmosphere if the exosphere is not protected by a strong magnetic field and stretches above the magnetopause, or from the polar regions. In such a case, exospheric neutral atoms can interact with the stellar plasma environment. Also, planetary ions can be detached from an ionopause by plasma instabilities in the form of ionospheric clouds (Terada et al. 2002).

In this section we present our estimations of ion pick-up loss, which is one of the most effective among non-thermal escape processes (according to analysis of data for Venus and Mars obtained by the Analyzer of Space Plasma and Energetic Atoms (ASPERA) instruments on board Venus Express and Mars Express). We assume the exoplanets have no magnetic field to estimate the maximum possible losses. In our model, the ions are produces by charge-exchange with stellar protons, photoionization by stellar photons and electron impact ionization by electrons in the stellar wind.

Charge exchange reactions between stellar wind protons and neutral planetary particles consist of the transfer of an electron from a neutral atom to a proton leaving a cold atmospheric ion and an energetic neutral atom (ENA). This process is described by the following reaction: $H_{sw}^{+} + H_{pl} \rightarrow H_{pl}^{+} + H_{ENA}$.

We used the Direct Simulation Monte Carlo (DSMC) method to model the stellar wind – upper atmosphere interaction. The code starts at an inner boundary R_0 where the Knudsen number is 0.1. The details about the initial algorithm can be found in Holmström et al. (2008) and further developed versions in Kislyakova et al. (2013, 2014). Here we summarize only the main procedure.

The code includes two species: neutral hydrogen atoms and protons. The following processes/forces can act on neutral H atoms:

- Collision with a UV photon, which can occur if the particle is outside of the planet's shadow. Leads to an acceleration of the hydrogen atom away from the star. A UV photon is absorbed by a neutral hydrogen atom and then consequently reradiated in a random direction, leading to a radial velocity change. The UV collision rate is velocity dependent (depends also on the star Lyman-α flux and distance to the planet).
- Ionization by a stellar photon (photoionization) or by a stellar wind electron.
- Charge exchange between neutral hydrogen atoms and stellar wind protons. If a hydrogen atom is outside the planetary obstacle (magnetopause or ionopause) it can charge exchange with a stellar wind proton. The charge exchange cross-section is taken to equal 2×10^{-19} m^2 (Lindsay and Stebbings 2005).
- Elastic collision with another hydrogen atom. Here the collision cross section was taken to be 10^{-21} m^2 (Izmodenov et al. 2000).

The coordinate system is centered at the center of the planet with the x-axis pointing towards the center of mass of the system, the y-axis pointing in the direction opposite to the planetary motion, and the z-axis pointing parallel to the vector Ω representing the orbital angular velocity of the planet. M_{st} is the mass of the planet's host star. The outer boundary of the simulation domain is the box $x_{min} \leq x \leq x_{max}$, $y_{min} \leq y \leq y_{max}$, and $z_{min} \leq z \leq z_{max}$. The inner boundary is a sphere of radius R_0.

Tidal potential, Coriolis and centrifugal forces, as well as the gravitation of the star and planet, acting on a hydrogen neutral atom are included in the following way (after Chandrasekhar 1963)

$$\frac{dv_i}{dt} = \frac{\partial}{\partial x_i}\left[\frac{1}{2}\Omega^2\left(x_1^2 + x_2^2\right) + \mu\left(x_1^2 - \frac{1}{2}x_2^2 - \frac{1}{2}x_3^2\right) + \left(\frac{GM_{st}}{R^2} - \frac{M_{st}R}{M_p + M_{st}}\Omega^2\right)x_1\right] + +2\Omega\epsilon_{il3}v_l \tag{7.6}$$

Here $x_1 = x$, $x_2 = y$, $x_3 = z$, v_i are the components of the velocity vector of a particle, G is Newton's gravitational constant, R is the distance between the centers of mass, ϵ_{il3} is the Levi-Civita symbol, and $\mu = GM_{st}/R^3$. The first term in the right-hand side of Eq. 7.6 represents the centrifugal force, the second is the tidal-generating potential, the third corresponds to the gravitation of the planet's host star

and the planet, while the last term stands for the Coriolis force. The self-gravitational potential of the particles is neglected.

Charge exchange takes place outside of an obstacle that corresponds to the magnetopause or ionopause boundary, which can be assumes as a surface described by

$$x = R_s \left(1 - \frac{y^2 + z^2}{R_t^2}\right). \tag{7.7}$$

Intensity of the stellar wind atmosphere erosion and, consequently, influence on the planetary evolution is different for different star ages and thus is strongly connected with the evolution of the star. It was discussed in Erkaev et al. (2013) and Kislyakova et al. (2013) that the stars of late spectral classes (red K and mostly M dwarfs) can keep high levels of the XUV radiation. The stellar wind evolution is more controversial (Wood et al. 2005), but higher XUV and X-ray heating intensify the non-thermal erosion of the atmosphere even if one considers the interaction with the constant stellar wind.

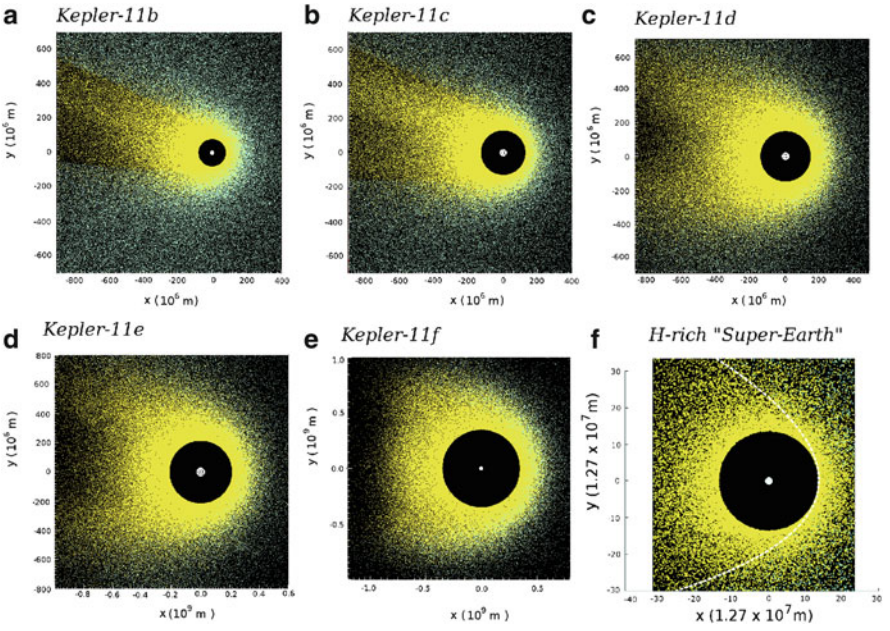

Fig. 7.3 **a**–**e**: Slices of modeled 3D atomic hydrogen coronae around the five Kepler-11 super-Earths for $-10^7 \leq z \leq 10^7$ m and heating efficiency $\eta = 40\,\%$. *Yellow* and *green dots* correspond to neutral hydrogen atoms and hydrogen ions, including stellar wind protons, respectively. The *white dot* in the center represents the planet. The *black empty area* around the planet corresponds to the XUV heated, hydrodynamically expanding thermosphere up to the height R_0 where Kn=0.1 (Kislyakova et al. 2013; 2014). **f**: Modeled atomic hydrogen coronae and stellar wind plasma interaction around a super-Earth hydrogen-rich planet inside an M star HZ at 0.24 AU. The XUV flux is 50 times higher than that of the present Sun, η=15 %; the *dashed line* denotes the planetary obstacle

Table 7.5 Ion pick-up loss rates and thermal escape rates for Kepler-11 planets for heating efficiency η (see Chap. 6, Shematovich et al. 2014) of 15 %. The values are given in [g·s^{-1}]. Thermal escape rates are taken from Table 3 in Lammer et al. (2013b)

Exoplanet	L_{ion}, η =15 %	L_{th}, η =15 %	L_{ion}, η =40 %	L_{th}, η =40 %
Kepler-11b	$\sim 1.17 \times 10^7$	$\sim 1.15 \times 10^8$	$\sim 1.3 \times 10^7$	$\sim 2.0 \times 10^8$
Kepler-11c	$\sim 1.07 \times 10^7$	$\sim 4.0 \times 10^7$	$\sim 1.37 \times 10^7$	$\sim 1.3 \times 10^8$
Kepler-11d	$\sim 1.47 \times 10^7$	$\sim 1.0 \times 10^8$	$\sim 2.33 \times 10^7$	$\sim 2.5 \times 10^8$
Kepler-11e	$\sim 1.84 \times 10^7$	$\sim 1.1 \times 10^8$	$\sim 3.34 \times 10^7$	$\sim 2.5 \times 10^8$
Kepler-11f	$\sim 6.0 \times 10^7$	$\sim 4.0 \times 10^8$	$\sim 6.8 \times 10^7$	$\sim 4.5 \times 10^8$

Figure 7.3 presents the results of the DSMC modeling of hydrogen coronae around five Kepler-11 super-Earths (Kislyakova et al. 2014) and around a test super-Earth with $M = 10M_\oplus$, $R = 2R_\oplus$ located in the HZ of an M dwarf (Kislyakova et al. 2013). As can be seen, in each case a huge hydrogen corona is formed composed of neutral hydrogen of planetary origin, ENAs and H atoms accelerated by the radiation pressure. Radiation pressure effects are of most importance in the vicinity of the host star (Kepler-11b and -c). This type of acceleration was considered by Bourrier and Lecavelier des Etangs (2013) and Lecavelier des Etangs et al. (2004) in application to the hot Jupiters, where these effects are of even higher importance.

In all cases, we considered non-magnetized planets, where the magnetic obstacle defined by Eq. 7.7 is located very close to the planets. Possible magnetic moments of exoplanets are discussed, for example, in Lammer et al. (2009b) and for Kepler-11b–f are believed to be rather weak. Table 7.5 illustrates average ion production rates, L_{ion}, depending on the heating efficiency η.

We found that in the Kepler-11 system the non-thermal loss rates are approximately one order of magnitude smaller than the thermal losses estimated for the same planets by Lammer et al. (2013a) (for detailed comparison and discussion see Kislyakova et al. (2014)). This ratio is in good agreement with results obtained by Kislyakova et al. (2013) and Erkaev et al. (2013) for an Earth-type planet and a super-Earth in the HZ of a GJ436-like M-type host star.

Conclusion

Thermal and non-thermal atmospheric escape rates from hydrogen-dominated upper atmospheres and their influence on atmospheric evolution of medium-size exoplanets are presented. The size, mass and distance to the planet's host star together with the stellar spectral type define in many aspects, if the planet may evolve into a terrestrial-type planet. The amount of initially accumulated gases, i.e. primordial nebula properties, plays also a big role (Lammer et al. 2014; Ikoma and Genda 2006). In general, close-in exoplanets lose their

(continued)

primordial envelopes and secondary atmospheres and reach the hydrodynamic blow off state much easier, and experience this escape condition longer (Lammer et al. 2013b), and they may lose their atmospheres also due to Roche-lobe overflow (Erkaev et al. 2007). At orbital distances of the HZ atmospheric evolution strongly depends also on the planet's mass and type of atmosphere. According to the results discussed in this chapter and in Lammer et al. (2014), Mars-sized bodies and planets with masses up to $<0.5 M_{\oplus}$ can lose a significant percentage or even the whole hydrogen-dominated protoatmosphere. On the other hand, so-called super-Earths will experience difficulties in losing their dense primordial envelopes composed mostly of light gases like hydrogen (Erkaev et al. 2013; Lammer et al. 2013b, 2014).

Non-thermal ion pick-up escape contributes to the total atmospheric losses as well, but although it is of most importance for small-sized planets like Mars (Lundin 2011), for bigger planets it makes up only several percent of total thermal and non-thermal losses and can not change the evolutionary scenarios significantly (Kislyakova et al. 2013, 2014).

Atmospheric evolution of an exoplanet is also deeply connected with the evolution of its host star. M dwarfs live longer and develop slower in comparison to Sun-type stars, which means that they stay longer in the very active XUV activity saturation phase (see also Chap. 1, Linsky and Güdel (2014). If an exoplanet orbits an M dwarf, it experiences severe stellar conditions (high levels of X-rays and EUV radiation, stronger stellar wind) much longer, leading to additional losses in comparison to an exoplanet of the same type orbiting a G star (Erkaev et al. 2013; Kislyakova et al. 2013).

Summarizing the above mentioned results, the evolution of a terrestrial-type nitrogen atmosphere requires several restrictions on an exoplanet and its host star. The star should be a long-lived object, which probably excludes the very early spectral classes; on the other hand, it should stay not too long in the highest XUV activity stage, when the planetary atmospheres undergo strong thermal and non-thermal atmospheric escape. The latter makes the fate of the exoplanets in M dwarf systems controversial, however, it is not excluded that the planets may evolve as a terrestrial-type body also orbiting these stars. As for the exoplanet itself, it has to be located in the right distance from its star, gain enough mass and volatiles during the formation. The volatile envelope should be thick enough to protect the atmospheres from the high stellar activity during the early age, but also thin enough to be lost. Otherwise the exoplanet would evolve into a mini-Neptune containing up to several percents of its weight as light gases.

Acknowledgements The authors acknowledge the support by the International Space Science Institute (ISSI) in Bern, Switzerland and the ISSI team *Characterizing stellar- and exoplanetary environments*. K. G. Kislyakova, and H. Lammer acknowledge support by the Austrian Research Foundation FWF NFN project S116 'Pathways to Habitability: From Disks to Active Stars, Planets

and Life', and the related FWF NFN subproject, 'Particle/Radiative Interactions with Upper Atmospheres of Planetary Bodies Under Extreme Stellar Conditions.'

References

Bourrier, V., & Lecavelier des Etangs, A. (2013). *Astronomy and Astrophysics, 557*, A124.
Broeg, C. H. (2009). *Icarus, 204*, 15.
Chandrasekhar, S. (1963). *Astrophysical Journal, 138*, 1182.
Elkins-Tanton, L. T., & Seager, S. (2008). *Astrophysical Journal, 685*, 1237.
Erkaev, N. V., Kulikov, Y. N., Lammer, H., Selsis, F., Langmayr, D., Jaritz, G. F., & Biernat, H. K. (2007). *Astronomy and Astrophysics, 472*, 329.
Erkaev, N. V., Lammer, H., Odert, P., Kulikov, Y. N., Kislyakova, K. G., Khodachenko, M. L., Güdel, M., Hanslmeier, A., & Biernat, H. (2013). *Astrobiology, 11*, 1–19.
Fossati, L., Haswell, C. A., Linsky, J. L., & Kislyakova, K. G. (2014). In H. Lammer & M. L. Khodachenko (Eds.), *Characterizing stellar and exoplanetary environments* (pp. 59). Heidelberg/New York: Springer.
Fridlund, F., Rauer, H., & Erikson, A. (2014). In H. Lammer & M. L. Khodachenko (Eds.), *Characterizing stellar and exoplanetary environments* (pp. 253). Heidelberg/New York: Springer.
Güdel, M. (2007). *Living Reviews in Solar Physics, 4*, 3.
Holmström, M. Ekenbäck, A. Selsis, F. Penz, T. Lammer, H. & Wurz, P. (2008). *Nature, 451*, 970–972.
Hunten, D. M., Pepin, R. O., & Walker, J. C. G. (1987). *Icarus, 69*, 532–549.
Ikoma, M., & Genda, H. (2006). *Astrophysical Journal, 648*, 696.
Izmodenov, V. V., Malama, Y. G., Kalinin, A. P., Gruntman, M. Lallement, R., & Rodionova, I. P. (2000). *APSS, 274*, 71–76.
Khodachenko, M. L., Ribas, I., Lammer, H., Grießmeier, J.-M., Leitner, M., Selsis, F., Eiroa, C., Hanslmeier, A., Biernat, H. K., Farrugia, C. J., & Rucker, H. O. (2007). *Astrobiology, 7*, 167–184.
Kislyakova, K. G., Lammer, H., Holmström, M., Panchenko, M., Odert, P., Erkaev, N. V., Leitzinger, M., Khodachenko, M. L., Kulikov, Y. N., Güdel, M., Hanslmeier, A. (2013). *Astrobiology, 11*, 1030–1048.
Kislyakova, K. G., Johnstone, C. P., Odert, P., Erkaev, E. V., Lammer, H., Lüftinger, T., Holmström. M., Khodachenko, M. L., & Güdel, M. (2014). *Astronomy and Astrophysics, 562*, A116.
Kulikov, Yu. N., Lammer, H., Lichtenegger, H. I. M., Terada, N., Ribas, E., Kolb, C., Langmayr, D., Lundin, R., Guinan, E. F., Barabash, S., & Biernat, H. B. (2006). *PSS, 54*, 1425.
Kulow, J. R., France, K., Linsky, J., & Parke Loyd, R. O. (2014), *Astrophysical Journal, 786*, 132 (9pp)
Lammer, H., Bredehöft, J. H., Coustenis, A., Khodachenko, M. L., Kaltenegger, L., Grasset, O., Prieur, D., Raulin, F., Ehrenfreund, P., Yamauchi, M., Wahlund, J.-E., Grießmeier, J.-M., Stangl, G., Cockell, C. S., Kulikov, Y. N., Grenfell, J. L., & Rauer, H. (2009a). *Astronomy and Astrophysics Review, 17*, 181–249.
Lammer, H., Odert, P., Leitzinger, M., Khodachenko, M. L., Panchenko, M., Kulikov, Y. N., Zhang, T. L., Lichtenegger, H. I. M., Erkaev, N. V., Wuchterl, G., Micela, G., Penz, T., Biernat, H. K., Weingrill, J., Steller, M., Ottacher, H., Hasiba, J., & Hanslmeier, A. (2009b). *Astronomy and Astrophysics, 506*, 399.
Lammer, H., Kislyakova, K. G., Güdel, M., Holmström, M., Erkaev, N. V., Odert, P., & Khodachenko, M. L. (2013a). In J. M. Trigo-Rodriguez, F. Raulin, C. Muller & C. Nixon (Eds.), *The early evolution of the atmospheres of terrestrial planets*. Astrophysics and space science proceedings (p. 33). New York: Springer.

Lammer, H., Erkaev, N. V., Odert, P., Kislyakova, K. G., Leitzinger, M., & Khodachenko, M. L., (2013b). *Monthly Notices of the Royal Astronomical Society, 430*, 1247–1256.

Lammer, H., Erkaev, N. V., Odert, P., Kislyakova, K. G., Leitzinger, M., & Khodachenko, M. L. (2014). *Monthly Notices of the Royal Astronomical Society, 439*, 3225.

Lecavelier des Etangs, A., Vidal-Madjar, A., McConnell, J. C., & Hébrard, G. (2004). *Astronomy and Astrophysics, 418*, L1-L4.

Lecavelier des Etangs, A., Pont, F., Vidal-Madjar, A., & Sing, D. (2008). *Astronomy and Astrophysics, 481*, L83.

Lecavelier des Etangs, A., Ehrenreich, D., Vidal-Madjar, A., Ballester, G. E., Désert, J.-M., Ferlet, R., Hébrard, G., Sing, D. K., Tchakoumegni, K.-O., & Udry, S. (2010). *Astronomy and Astrophysics, 514*, A72.

Leitzinger, M., Odert, P., Kulikov, Y. N., Lammer, H., Wuchterl, G., Penz, T., Guarcello, M. G., Micela, G., Khodachenko, M. L. Weingrill, J. Hanslmeier, A. Biernat, H. K., & Schneider, J., (2011). *PSS, 59*, 1472.

Lichtenegger, H. I. M., Lammer, H., Grießmeier, J.-M., Kulikov, Y. N., von Paris, P., Hausleitner, W., Krauss, S., & Rauer, H. (2010). *Icarus, 210*, 1.

Lindsay, B. G. & Stebbings, R. F. (2005). *Journal of Geophysical Research, 110*, 12213.

Linsky, J. L., & Güdel, M., (2014). In H. Lammer & M. L. Khodachenko (Eds.), *Characterizing stellar and exoplanetary environments* (pp. 3). Heidelberg/New York: Springer.

Lundin, R. (2011). *SSR, 162*, 309.

Mordasini, C., Alibert, Y., Georgy, C., Dittkrist, K.-M., & Henning, T. (2012). *Astronomy and Astrophysics, 545*, A112.

Shematovich, V. I., Bisikalo, D. V., & Dmitry E. I. (2014). In H. Lammer & M. L. Khodachenko (Eds.), *Characterizing stellar and exoplanetary environments* (pp. 105). Heidelberg/New York: Springer.

Tian, F., Kasting, J. F., Liu, H.-L., & Roble, R. G. (2008a). *Journal of Geophysical Research, 113*, 5008.

Tian, F., Solomon, S. C., Quian, L., & Lei, J. (2008b). *Journal of Geophysical Research (Planets), 113*, 7005.

Terada, N., Machida, S., & Shinagawa, H. (2002). *Journal of Geophysical Research (Space Physics), 107*, 1471.

Vidal-Madjar, A., Lecavelier des Etangs, A., Désert, J.-M., Ballester, G. E., Ferlet, R., Hébrard, G., & Mayor, M. (2003). *Nature, 422*, 143.

Wood, B. E., Müller, H.-R., Zank, G. P., Linsky, J. L., & Redfield, S. (2005). *Astrophysical Journal Letters, 628*, L143.